Transactions of the Nigerian Association of Mathematical Physics
Volume 3, (January, 2017), **pp 255 – 262**

Comparative Investigation of Specific Energy Absorption Rate on Biological Tissues Using Field Measurement and Computational Analysis

[1]Ushie P.O., [1]Pekene D.B, [1]Edet C.O. and [2]Inyang E.P.

[1]Department. of Physics, Cross River University of Technology, Calabar, Nigeria.
[2]Department of Physics, University of Calabar, Calabar, Nigeria.

Abstract

In this article, computational analysis and field measurement evaluation in studying the Specific Absorption Rate (SAR) of Electromagnetic radiation on selected biological tissues was carried out. The possible penetrating and harmful effects influenced by an electromagnetic radiation into human tissues due to mobile phones was critically analysed. In order to effectively estimate and analyse the electric field and SAR within the human head, mathematical models which combines Green's function analysis of the human head modeled by a double-layered sphere and Electric Field Integral Equation (EFIE) was considered. Specifically, the effects at Universal Mobile Telecommunication System(UMTS) operating frequency of 2155MHz and gap distances of 0.5cm to 4.0cm at an interval of 0.5cm between the mobile phone and the human head was the focus. It was observed from the results that calculated penetrated electric field transmitted from the mobile phone and the corresponding SAR values is decreased by about 90% if the mobile phone moves from 0.5cm to 4cm away from the body. Also from the results, it is found that the trend of theoretically obtained SAR curve was smoothly decaying exponentially as distance increased and that of experimental was not smooth but SAR decreased with increase in distance. A correlation coefficient of approximately 0.8 was obtained for all three tissues in both theory and experimental result of SAR evaluated. From this study, this may imply that by increasing the distance between human head and mobile phone, the effect of absorbed Radio Frequency-Electromagnetic Field radiations can be rendered insignificant.

Keywords: EFIE, Electric field strength, Green's function, Human Tissue, Penetration Depth, Radiation, and SAR

1.0 Introduction

The rate at which radio frequency (RF) hazard which is caused by electromagnetic absorption is becoming very alarming and it corresponding effect needs not be overemphasized. Electromagnetism (EM), the force that lights up our cities; Lasers, radio, TV, modern electronics, computers, the internet, electricity, magnetism-all are consequences of the electromagnetic force. It is perhaps the most useful force harnessed by humans [1]. Extensive usage of mobile phones and other personal communication devices are the main sources of electromagnetic radiation and absorption.

In chorus with the expanding usage, a question has been raised repeatedly as to whether frequent usage of such a device which radiates GHz electromagnetic field on the head is unsafe. The rapid expansion has thus pushed the research towards the necessity of analyzing mobile phones for radiation performance to address the safety concern [2].

The effect of mobile phone radiation on human health is a subject of interest and studied worldwide, as a result of the enormous increase in mobile phone usage throughout the world.

In May 2011, the World Health Organization's International Agency for Research on Cancer announced electromagnetic fields from mobile phones and other sources as "possibly carcinogenic to humans" and advised the public to adopt safety measures to reduce exposure, like use of hands-free devices or texting.

Corresponding author: Ushie P.O., E-mail: patushie98@gmail.com, Tel.: +2348065324848

As of 2016, Sony Ericson mobile Communications Company asserted that there were 7.4 billion subscriptions worldwide (but some have more than two, so 4,230 million users in 2014 gives a better picture with about 97 phones per 100 citizens).
The electromagnetic radiation used by mobile phones operates in the microwave range (450-2100MHz). The method generally used to access the radiation of mobile phones is the specific absorption rate (SAR), this is an indication of the amount of electromagnetic energy absorbed by biological tissues. The specific absorption rate measured in watts per kilogram (W/kg) is the fundamental RF dosimetry parameter and is defined as the rate of energy absorbed per unit mass. The SAR is defined by the incident electromagnetic waves and by the electrical and geometrical characteristics of the exposed object [3].
Electromagnetic radiation is a transversal wave motion propagating at the speed of light. It is created by an accelerating or decelerating electrical charge. The radiation is characterized by its frequency f and wavelength λ, which are connected by;

$$\mathbf{f} = \frac{c}{\lambda} \quad (1)$$

where C is the velocity of light in vacuum. In a general case the speed of the wave V is determined by the properties of the medium and it can be calculated by

$$V = \frac{1}{\sqrt{\varepsilon\mu}} \quad (2)$$

Where ε and μ are the permittivity and permeability of the medium, respectively.
The spectrum of electromagnetic radiation is subdivided into groups depending on frequency and wavelength [4]. Radio waves are located at the lower end of the frequency scale, ranging up to about 3 THz as presented in Fig. 1. This Research work deals mainly with microwaves from 300 MHz to 3 GHz [5].

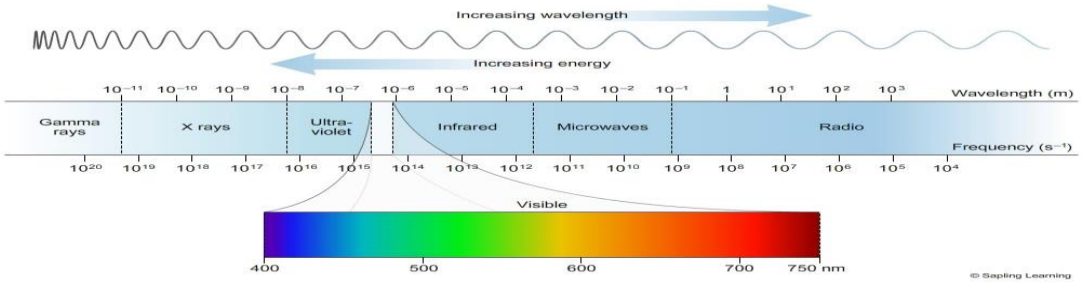

Fig. 1; Electromagnetic Spectrum (6)
The following expressions describe the electric type Green's function in the three regions of space. The geometry of the problem is depicted in Fig.2.

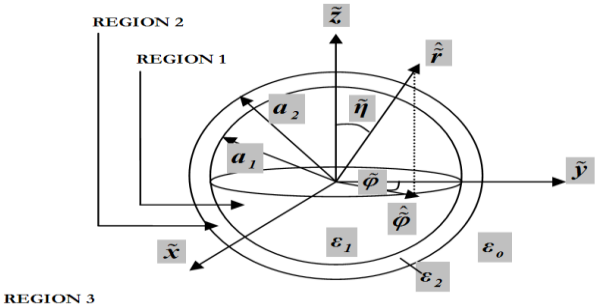

Fig. 2: The geometry of the problem
The head is modeled by a double-layered sphere with radii a_1 anda_2. The two layers are used to simulate different biological media; bone and brain (gray matter) tissues. The regions (1) and (2) have dielectric constants ε_1 and ε_2 respectively. The region (3) represents the free space with dielectric constant, ε_0. The system is excited by an antenna placed outside the head model where the antenna's axis is considered parallel to z-axis. Green's function in each region i=1, 2, 3 of space is properly expanded to an infinite sum of spherical waves satisfying the appropriate vector wave equation. By virtue of the spherical symmetry of the problem, spherical coordinates are used, with unit vectors $\hat{r}$, $\hat{n}$ and $\hat{\varphi}$. By the mathematical property of spherical symmetry of the problem, spherical co-ordinates are used, with unit vector $\hat{r}, \hat{n}, \hat{\varphi}$ just as $(\hat{r}, \hat{\theta}, \hat{\phi})$. The following expansions describe the electric type Green's function in the three regions of space.

Region 1

$$\overline{\underline{G}}_1(\tilde{r}, \tilde{r}') = \sum_{n=1}^{\infty}\sum_{m=-n}^{n}\left[\underline{m}_{mn}^{(1)}(\underline{\tilde{r}}, k_1)\,\underline{a}_{mn}(\underline{\tilde{r}}') + \underline{n}_{mn}^{(1)}(\underline{\tilde{r}}, k_1)\,\underline{a}'_{mn}(\underline{\tilde{r}}')\right].$$

$$\tilde{r} \leq a_1. \quad (3)$$

Region 2

$$\overline{\underline{G}}_2(\tilde{r}, \tilde{r}') = \sum_{n=1}^{\infty}\sum_{m=-n}^{n}\left[\left(\underline{m}_{mn}^{(1)}(\underline{\tilde{r}}, k_2)\,\underline{b}_{mn}(\underline{\tilde{r}}') + \underline{n}_{mn}^{(1)}(\underline{\tilde{r}}, k_2)\,\underline{b}'_{mn}(\underline{\tilde{r}}')\right) + \left(\underline{m}_{mn}^{(2)}(\underline{\tilde{r}}, k_2)\,\underline{c}_{mn}(\underline{\tilde{r}}) + \underline{n}_{mn}^{(2)}(\underline{\tilde{r}}, k_2)\underline{c}'_{mn}(\underline{\tilde{r}}')\right)\right],$$

$\tilde{r} \leq a_2$. (4)

Where $k_i = k_0\sqrt{\varepsilon_i}$, $\underline{a}_{mn}(\tilde{r}')$, $\underline{a}'_{mn}(\tilde{r}')$…., $\underline{c}'_{mn}(\tilde{r}')$ are unknown coefficients to be determined and $\underline{m}^{(j)}_{mn}(\tilde{r}', k_i)$, $\underline{n}^{(2)}_{mn}(\tilde{r}', k_i)$, I = 1, 2,3 ; j =1, 2, 3 are the well-known spherical harmonics wave functions. Regarding, the region outside the head and inside the ellipsoidal cavity, the electric field consists of the primary excitation $\overline{G}_0(\tilde{r}, \tilde{r}')$ from the unit source located at $\underline{\tilde{r}}'$ and the contribution of the field $\overline{G}_s(\tilde{r}, \tilde{r}')$, scattered from the double layered sphere. Thus,

Region 3

$\overline{G}_3(\tilde{r}, \tilde{r}') = \overline{G}_0(\tilde{r}, \tilde{r}') + \overline{G}_s(\tilde{r}, \tilde{r}')$ (5)

where $\overline{G}_0(\tilde{r}, \tilde{r}')$ is the free space dyadic Green's function and is defined by an infinite sum spherical waves as

$$\overline{G}_0(\tilde{r}, \tilde{r}') = \sum_{n=1}^{\infty}\sum_{m=-n}^{n}(-1)^m \frac{jk_o}{4\pi}\frac{2n+1}{n(n+1)} \times \begin{cases} \underline{m}^{(1)}_{-mn}(\underline{\tilde{r}}', k_0)\underline{m}^{(3)}_{mn}(\underline{\tilde{r}}, k_o) + \underline{n}^{(1)}_{mn}(\underline{\tilde{r}}, k_0)\underline{n}^{(3)}_{mn}(\underline{\tilde{r}}', k_0), \tilde{r} > \tilde{r}' \\ \underline{m}^{(3)}_{-mn}(\underline{\tilde{r}}', k_0)\underline{m}^{(1)}_{mn}(\underline{\tilde{r}}, k_0) + \underline{n}^{(3)}_{mn}(\underline{\tilde{r}}, k_0)\underline{n}^{(1)}_{mn}(\underline{\tilde{r}}', k_0), \tilde{r} < \tilde{r}' \end{cases} \quad (6)$$

Hereupon, the unknown expansion coefficients of the infinite sum of spherical waves are determined by the boundary conditions on the interfaces $\tilde{r} = a_1, a_2$. In order to satisfy the continuity of the tangential electric and magnetic field components, the boundary conditions on the interfaces $\tilde{r} = a_1, a_2$ are then imposed by implementing the expressions:

$\hat{\tilde{r}} \times \overline{G}_{i+1}(\underline{\tilde{r}}, \underline{\tilde{r}}') = \hat{\tilde{r}} \times \overline{G}_{i+1}(\underline{\tilde{r}}, \underline{\tilde{r}}')$. $\tilde{r}=a_i$ (7)

I= 1, 2

$\hat{\tilde{r}} \times \left(\nabla \times \overline{G}_i(\underline{\tilde{r}}, \underline{\tilde{r}}')\right) = \hat{\tilde{r}} \times \left(\nabla \times \overline{G}_{i+1}(\underline{\tilde{r}}, \underline{\tilde{r}}')\right)$. (8)

$\tilde{r}=a_i$ I =1, 2

Where $\hat{\tilde{r}}$ denotes the unit vector along the radial direction of the local coordinate system. By implementing the orthogonality properties of the spherical harmonics wave functions, two independent 4 X 4 linear sets of equations are obtained for the unknown expansion coefficients stated above [7].

2.0 Electric-field Integral Equation

The electric-field integral equation (EFIE) is a relationship that allows the calculation of an electric field (E) generated by an electric current (J).

When all quantities in the frequency domain are considered, a time dependency $e^{+j\omega t}$ that is suppressed throughout is assumed. Beginning with the Maxwell equations relating the electric and magnetic field an assuming linear, homogeneous media with permeability μ and permittivity ϵ :

$\nabla \times E = -j\omega\mu H$. (9)

$\nabla \times H = j\omega\epsilon + J$. (10)

Following the third equation involving the divergence of H

$\nabla . H = 0$. (11)

by vector calculus, we can write any divergence less vector as the curl of another vector,

Hence

$\nabla \times A = H$. (12)

Where A is called the magnetic vector potential. Substituting this into the above we get

$\nabla \times (E + j\omega\mu A) = 0$. (13)

And any curl-free vector can be written as the gradient of a scalar, hence

$E + j\omega\mu A = -\nabla\phi$. (14)

where ϕ is the electric scalar potential; these relationships now allow us to write:

$\nabla \times \nabla \times A - k^2 A = J - j\omega\varepsilon\nabla\phi$. (15)

where $k = \omega\sqrt{\mu\varepsilon}$, which can be re-written by vector identity as

$\nabla \times (\nabla . \mathrm{A}) - \nabla^2 \mathrm{A} - \mathrm{k}^2 \mathrm{A} = \mathrm{J} - \mathrm{j}\omega\varepsilon\nabla\phi$. (16)

As we have only specified the curl of A, we're free to define the divergence, and choose the following:

$\nabla . A + k^2 A = -J$. (17)

which is the vector Helmholtz equation. The solution of this equation for A is

$A(r) = \frac{1}{4\pi}\iiint J(r')G(r, r')\, dr'$. (18)

Where $G(r, r') = \frac{e^{(-jk)|r-r'|}}{|r-r'|}$. (19)

We can now write what is called the electric field integral equation (EFIE), relating the electric field E to the vector potential A

$E = -j\omega\mu A + \frac{1}{j\omega\varepsilon}\nabla(\nabla . A)$. (20)

We can now further represent the EFIE in the dyadic form as

$$E = -j\omega\mu \iiint dr' G(r,r')\, J(r'). \quad (21)$$

Where $G(r,r')$ here is the dyadic homogenous Green's function given by:

$$G(r,r') = \frac{1}{4\pi}\left[\mathrm{I} + \frac{\nabla\nabla}{\mathrm{k}^2}\right] G(r,r'). \quad (22)$$

The EFIE describes a radiated field $\vec{E}$ given a set of sources J, and as such it is the fundamental equation used in antenna analysis and design. It is a very general relationship that can be used to compute the radiated field of any sort of antenna once the current distribution on it is known.

The most important aspect of the EFIE is that it allows us to solve the radiation/scattering problem in an unbounded region, or one whose boundary is located at infinity. In scattering problems, it is desirable to determine an unknown scattered field E_s that is due to a known incident field E_i .

Unfortunately, the EFIE relates the scattered field to **J**, not the incident field, so we do not know what **J** is. This sort of problem can be solved by imposing the boundary conditions on the incident and scattered field, allowing one to write the EFIE in terms of E_i and **J** alone. Once this has been done, the integral equation can then be solved by a numerical approach using the method of moments [8].

The EFIE is a Fredholm integral equation of the first kind, where the current appears inside the integral sign only. Because the derivation did not impose any constraint on the shape of the scatterer, the EFIE may be applied to closed surfaces as well as open, thin objects. For thin surfaces, the current $J(r)$represents the vector sum of the current density on both sides of the scatterer [9].

3.0 Cellular Telephone Specific Absorption Rate (SAR)

SAR is a value that corresponds to the relative amount of RF energy absorbed in the head of a user of a wireless handset. The FCC limit for public exposure from cellular telephones is at SAR level of 1.6 watts per kilogram (1.6W/kg)

European Union: CENELEC specified SAR limits within the EU, following IEC standards. For mobile phones, and other such hand-held devices, the SAR limit is 2 W/kg averaged over the 10 g of tissue absorbing the most signal (IEC 62209-1).

India: switched from the EU limits to the US limits for mobile handsets in 2012. Unlike the US, India will not rely solely on SAR measurements provided by manufacturers; random compliance tests are done by a government-run Telecommunication Engineering Center (TEC) SAR Laboratory on handsets and 10% of towers. All handsets must have a hands free mode.

SAR for electromagnetic energy can be calculated from the electric field within the tissue as:

$$SAR = \frac{\sigma(r)|E(r)|^2}{2\rho(r)}. \quad (23)$$

σ is the electrical conductivity, E is the root mean square electric field, ρ is the density and V is the volume

SAR measures exposure to fields between 100 KHz and 10 GHz (known as radio waves) [10]. It is commonly used to measure power absorbed from mobile phones and during MRI scans. The value will depend heavily on the geometry of the part of the body that is exposed to the RF energy and on the exact location and geometry of the RF source. Thus tests must be made with each specific source, such as a mobile phone model, and at the intended position of use.

Body tissue dielectric parameters**:** The following tissue dielectric parameters are computed according to the 4-cole-cole model [11] described in compilation of the dielectric properties of body tissues at RF and microwave frequencies by Camelia Gabriel in the U.S. air force report (Table 1).

Table 1: Body tissue dielectric properties at 2155 MHz

Tissue	Permittivity(F/m)	Density(kg/m^3)	Conductivity(S/m)
Avg. Brain	42.970322	1030.0	1.340520
Avg. Skull	15.227116	1850.0	0.520847
Avg. Muscle	53.962143	1040.0	1.607689

Fig. 3: A phantom model of the human showing a quasi-view of the experimental setup.

4.0 Method

An empty room was selected for the electric field measurements to be carried out, at least it was 90% free of other EM radiation sources , this was done in other to avoid conflicting values and ambiguity. A mobile phone placed at 0.5cm from the broadband metre(Electrosmog, ED 78S model) and the electric field at that point was noted and for subsequent values at 1.0 cm, 1.5 cm, 2.0 cm…4.0 cm. Electric field values noted at different distances were also obtained through the use of the broadband metre and a metre rule for noting various distances. A phantom head model is presented in Fig. 3.

Referring to Eq. 22 and Table 1 various values of SAR where calculated. Software called "power estimator" was used to generate electric field values which was also used to calculate SAR, this values served as the theoretically obtained values for SAR.

5.0 Result

Table 2: Theoretically obtained values.

E (V/m)	Distance=L±0.05cm	Brain SAR	Skull SAR	Muscle SAR
7889	0.50	40499.53	8760.973	
3944	1.00	10122.32	2189.688	12022.9909
2630	1.50	4501.089	973.6883	5346.26156
1972	2.00	2530.579	547.422	3005.74772
1578	2.50	1620.392	350.5278	1924.65416
1315	3.00	1125.272	243.4221	1336.56539
1127	3.50	826.521	178.7954	981.717511
986	4.00	632.7782	136.8844	751.595457

Table 3: Experimentally obtained values

E(V/m)	Distance=L±0.05cm	Brain SAR	Skull SAR	Muscle SAR
1.425	0.50	0.001321405	0.00028585	0.001569526
1.346	1.00	0.001178952	0.000255034	0.001400325
0.975	1.50	0.000618608	0.000133819	0.000734764
0.964	2.00	0.000604728	0.000130816	0.000718278
0.74	2.50	0.000356344	7.70854E-05	0.000423255
0.574	3.00	0.000214403	4.63802E-05	0.000254661
0.504	3.50	0.000165298	3.57577E-05	0.000196336
0.104	4.00	7.03838E-06	1.52256E-06	8.35998E-06

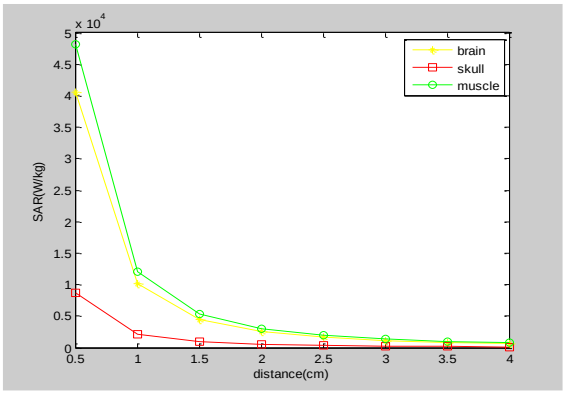

Fig. 4: SAR against Distance from theoretical values obtained.

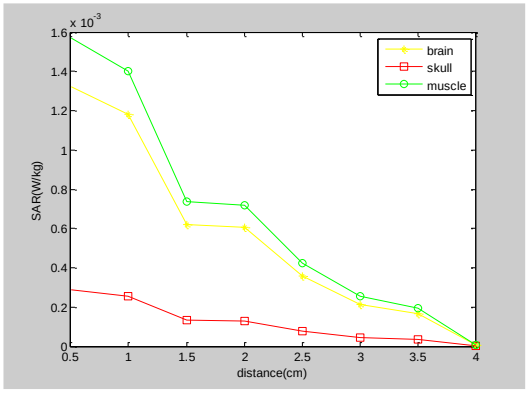

Fig. 5: SAR against Distance from Experimental values

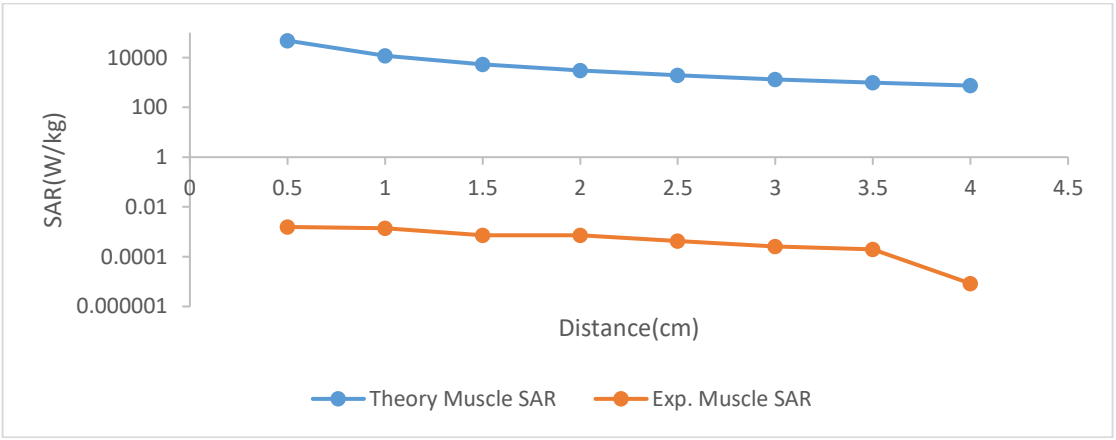

Fig. 6: Correlation plot of theoretical and experiment on muscle SAR versus distance.

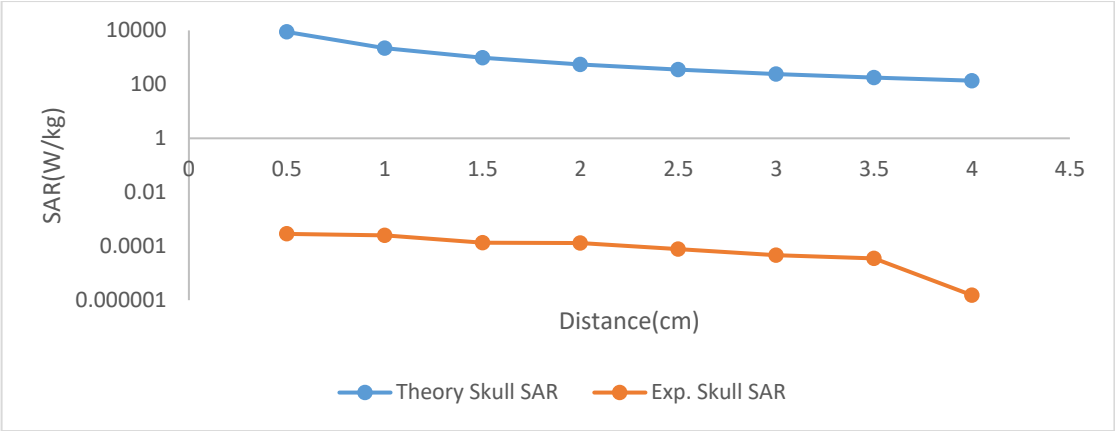

Fig. 7: Correlation plot of theoretical and experiment on Skull SAR versus distance.

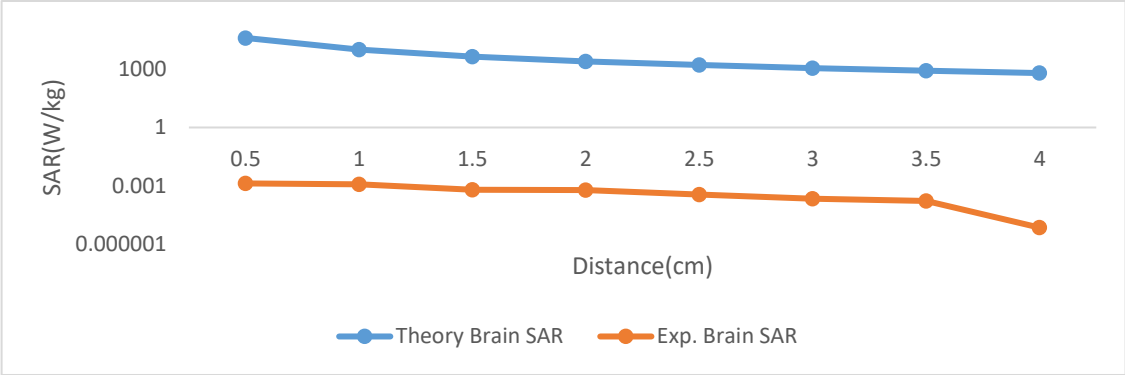

Fig. 8: Correlation plot of theoretical and experiment on Brain SAR versus distance.

6.0 Discussion

From Table 4.0 and Figure 4.0 respectively, the results obtained theoretically shows that as distance increases SAR values decreases for all three selected biological tissues which is in consonance with literature [10,11, 12 and 13] At point 0.5cm, the mobile phone was very close to the human head, and more energy is absorbed. At this point, muscle had more absorption rate than other tissues followed by brain and the least was the skull. SAR values continuously depreciates for all tissues and at points 1.0cm, 1.5cm, 2.0cm and 2.5cm though muscle SAR was still higher than that of other tissues. At these four points, the trend for skull and brain SAR were approximately the same. From 3.0cm up to 4.0cm for the three biological tissues the curves died off exponentially and in unison without any lagging and any leading with any value up to 10%.

From Figure 4.1 and Table 4.1, muscle has the highest SAR values although there is an exception at a certain point (i.e. 4cm) where all the curves converged and the SAR values for all three biological tissues were approximately equal as it dropped to almost zero. At point 0.5cm muscle SAR was higher and followed by brain and skull respectively and at point 1.0 cm it decreased in the same order up to point 2.5cm. At point 3.0cm, 3.5cm and at 4.0cm there was a decline which occurred uniformly in all three tissues. But one thing was obvious in Figure 4.1 which is the fact that the curves were not smoothly decaying unlike the case observed in Figure 4.0. This is attributed to possible EM radiation hot spot that could be present. Muscle SAR was also far higher in both cases because it is believed that from anatomical/physiological arrangement of the human body tissue, the muscle precedes the skull and then the brain comes last. As the field penetrated further, the field faded away along the distance $1/xk_o$ to a value 1/e of the original value. This is in agreement with the concept of penetration depth or skin depth, and it is also the reason behind the brain and skull having relatively less values compared to muscle. But absorption in skull was less because it has a high density ($1850Kg/m^3$), so EM field cannot permeate such tissue easily. Compared to other biological tissues (i.e. Muscle and brain) skull SAR was less than all and this is consistent with concept depicted in the former (i.e. as density increases SAR decreases).

Figure 4.2, 4.3 and 4.4 explicitly shows a correlation plot of theoretical SAR values and experimental SAR values of each of the three biological tissues against distance. From the plot it is seen that experimental values had extremely low values compared to theory. The correlation coefficient obtained thereof was approximately 0.8 for each biological tissue, which indicates that there is a positive and good relationship between the SAR theory and SAR experimental obtained and the trend as seen in all the three correlation plots shows decrease in SAR with distance.

7.0 Conclusion

Calculation was done using theoretical(computational) and experimental approach, values obtained from experiment falls far below the exposure limits given by ICNIRP and FCC respectively, and that obtained from theory was large, but there is no cause for alarm since theory is actually an ideal case and our goal is actually the trend of the plot. But experimental values are preferred because they are more realistic absorption rates for the human body tissues. We found out that as the field penetrated further, the field faded away along the distance $1/xk_o$ to a value 1/e of the original value. This is in agreement with the concept of penetration depth or skin depth, and it is also the reason behind the brain and skull having relatively less values compared to muscle. We also discovered that absorption in skull was less because it has a high density ($1850Kg/m^3$), so EM field cannot permeate such tissue easily. Compared to other biological tissues (i.e. Muscle and brain) skull SAR was less than all

8.0 Acknowledgement

The authors wish to express their sincere gratitude to Irene Karanasiou for making her article accessible to all as that assisted in giving us an access to the spherical head model of the human head.

9.0 References

[1]. Kaku, Michio (2008). Physics of the Impossible (1st ed.). New York: Double Day. ISBN 978-0-385-52069-0. *P. 6-7*

[2]. Wiart J.,Hadjem A ,Wong M F and Bloch I(2008),Analysis of RF exposure in the head tissues of children and adults. IOP Publishing. P. 200-210

[3]. Gandhi, O.P. Lazzi, G. Furse, C.M(1996), Electromagnetic absorption in the human head and neck for mobile telephones at 835 and 1900 MHz, IEEE Transactions on Microwave Theory and Techniques, Vol. 44(10), P. 1884-1897.

[4]. Räisänen A. V.,Lehto A.(2003): Radio Engineering for Wireless Communication and Sensor Applications, Artech House (Boston, Massachusetts), P. 396. http://dx.doi.org/10.4314/njt.v34i2.20

[5]. Islam Ahmed Abdul Maksoud Ali Soliman.(2009) .Application of Dyadic Green's Function Method in Electromagnetic Propagation Problems.(A Thesis Presented to the Graduate School Faculty of Engineering, Alexandria University In Partial Fulfillment of the Requirements for the Degree Of Master of Science). P. 10

[6] http://sites.google.com/site/chempendix/em-spectrum

[7]. Irene Karanasiou(2014), SAR estimation in human head models related to TETRA, GSM and UMTS exposure using different computational approaches, WSEAS TRANSACTIONS on BIOLOGY and BIOMEDICINE, Vol. 11, P. 101-110

[8]. Rao , Wilton, Glisson (1982) . Electromagnetic Scattering by surfaces of Arbitrary Shape. IEEE Transactions on Antennas and Propagation , Vol, AP-30, No.3. doi:10.1109/TAP.1982.1142818 P. 15-18.

[9]. Thomas G. and Finney R. (1992), Calculus and Analytic Geometry. Addison-Wesley. P. 124.

[10]. ICNIRP(1998), Guidelines for limiting exposure to time-varying electric, magnetic, and electromagnetic fields (up to 300 GHz), Health Physics. Vol. 74(4), P. 494 – 522,

[11] www.fcc.gov/general/body-tissue-dielectric-parameters

[12] Sabar A. A. and Jabir S. A. (2013). SAR Simulation in Human Head Exposed to RF signals and safety precautions. International Journal of Computer Science and Engineering Technology. Vol. 3 (9) P. 334-340

[13]. Ragha L.K. and Bhatia M.S. (2009). Numerical Evaluation of SAR for Compliance Testing of Personal Wireless Devices. International Journal of Recent Trends in Engineering, Vol. 2(6). P. 69-72

[14]. Joseph Isabona and Kingsley Obahiagbon (2015),Specific Absorption Rate and Temperature rise Computation in Human Tissues due to Electromagnetic Field emission from Mobile Phones at 900 MHz and 1800 MHz Computing, Information Systems, Development Informatics & Allied Research Journal 6(2). www.cisdijournal.net Vol. 6(2), P. 53-62